OFFICE OF NAVAL RESEARCH

GRANT or CONTRACT: N00014-91J-1201

R&T CODE: 4133032
Richard Carlin

TECHNICAL REPORT NO. 23

"Preparation and Stability of Template-Synthesized Metal Nanorod Sols in Organic Solvents"

by Veronica M. Cepak and Charles R. Martin

Published

in

Journal of Physical Chemistry

Colorado State University
Department of Chemistry
Fort Collins, CO 80523-1872

December 1, 1998

REPORT DOCUMENTATION PAGE

1. December 1, 1998

2. Interim report

3. "Preparation and Stability of Template-Synthesized Metal Nanorod Sols in Organic Solvents"

4. GRANT: N00014-91J-1201, R&T CODE: 4133032

5. Veronica M. Cepak and Charles R. Martin

6. Charles R. Martin, Department of Chemistry, Colorado State University, Fort Collins, CO 80523-1872

7. TECHNICAL REPORT NO. 23

8. Office of Naval Research, Chemistry Division, 800 North Quincy Street, Arlington, VA 22217-5660

9. Published in *J. Physical Chemistry*

10. Reproduction in whole or in part is permitted for any purpose of the United States Government. This document has been approved for public release and sale; its distribution is unlimited.

11. Abstract: Gold and silver nanorods of diameter 40 and 90 nm, and having a variety of aspect ratios (length/diameter), were prepared using the template synthesis approach. The stability of these nanorod sol was monitored using visible absorption spectroscopy. For both the Au and Ag nanorods (in both solvents), sols prepared from the 90 nm-diameter nanorods were found to be less stable than sols prepared from the 40 nm-diameter nanorods. The addition of the polymeric stabilizers poly(vinylpyridine) or poly(vinylpyrrolidone) did not enhance the stability of these nanorod sols.

12. Subject terms: Template synthesized, gold nanorod sols, silver nanorod sols, stability.

17. 18. 19. Unclassified

Preparation and Stability of Template-Synthesized Metal Nanorod Sols in Organic Solvents

Veronica M. Cepak and Charles R. Martin*

Department of Chemistry

Colorado State University

Fort Collins, CO 80523

*To whom correspondence should be addressed.

email: crmartin@lamar.colostate.edu

ABSTRACT

Gold and silver nanorods of diameter 40 and 90 nm, and having a variety of aspect ratios (length/diameter), were prepared using the template synthesis approach. After template synthesis, the nanorods were freed from the template membrane and dispersed in either hexafluoroisopropanol (HFIP) or $CHCl_3$. The stability of these nanorod sol was monitored using visible absorption spectroscopy. For both the Au and Ag nanorods (in both solvents), sols prepared from the 90 nm-diameter nanorods were found to be less stable than sols prepared from the 40 nm-diameter nanorods. The addition of the polymeric stabilizers poly(vinylpyridine) or poly(vinylpyrrolidone) did not enhance the stability of these nanorod sols. In addition, to these studies of sol stability, UV/visible absorption spectroscopy was used to investigate the plasmon absorption band of these sols. The wavelength of maximum absorbance of the plasmon resonance band (λ_{max}) for both Ag and Au sols was shifted to higher wavelengths when the nanorod diameter was increased from 40 nm to 90 nm. In addition, the λ_{max} values for sols prepared in $CHCl_3$ were redshifted relative to analogous sols prepared in HFIP.

INTRODUCTION

The template method for preparing nanomaterials entails synthesis of the desired material into the pores of a nanoporous membrane or other solid.[1,2] This method provides a convenient route for preparing rod-like (i.e., nonspherical) metal and other nanoparticles. The diameter of these rod-shaped nanoparticles (nanorods) can be varied by using template membranes with different pore diameters, and in the case of electrochemical metal deposition within the pores, the length of the nanorod can be changed by varying the quantity of charge used to deposit the metal.[2-4] Hence, the template method can be used to prepare metal and other nanorods with nearly any desired aspect ratio (length/diameter).[3,4]

There has been recent interest in preparing colloidal dispersions of such nanorods.[5-7] One motivation for this work is the possibility of self-assembling such nanorods, from the colloidal dispersion, to make organized structures, where the nanorods are the building blocks of the structure. In this paper we investigate the possibility of preparing colloidal dispersions of metal (Au and Ag) nanorods in the organic solvents hexafluoroisopropanol (HFIP) and $CHCl_3$. Procedures for preparing such dispersions are described, and results of experiments aimed at probing the stability of these dispersions are presented.

EXPERIMENTAL

Template-Synthesis of the Metal Nanorods. Track-etched polycarbonate filtration membranes (nominal pore diameters of 10 nm and 30 nm) were obtained from Poretics and Corning. These membranes were 6 μm

thick and had a reported pore density of 6 x 10^8 pores cm^{-2}. The Au and Ag nanorods were deposited into the pores of these membranes by electrochemical reduction of a solution of the desired metal ion. However, prior to electrodeposition of the metal, the template membrane was "sensitized" by immersion into a solution of Sn^{2+}; we have used the same Sn^{2+}-sensitization process prior to electroless deposition of Au within the pores of these membranes.[8-10] The reagents were used as received and have been reported in these prior publications. Sensitization in this way was found to greatly improve the reproducibility of the electrochemical deposition of Au and Ag into the pores of these membranes. Milli Q 18-MΩ was used for rinsing and for all aqueous solutions.

After sensitization[8-10] the membranes were rinsed with CH_3OH (ACS grade, Fisher Scientific), dried in air, and used immediately. In order to electrochemically deposit metal into the pores of these membranes, a cathode must be applied to one face of the membrane. This was accomplished by evaporating Ag (Aldrich, 99.9+%) using a Denton Vacuum DV502A evaporator; the Ag-film cathode obtained was ~0.5 μm thick. The template membrane was then clamped between an ITO-glass slide (PPG Industries) and a section of glass tubing (30 mm diameter) which terminated with an O-ring joint. The tubing served as the electrochemical cell and the O-ring (45 mm diameter) determined the area of the template membrane into which the metal was deposited. The Ag-film cathode was placed downward so as to be in electrical contact with the ITO.

The metal nanorods were deposited into the pores using a previously reported constant-potential deposition method.[11-15] A Pt/Rh-gauze counter electrode (Alfa Aesar) and a Ag/AgCl reference electrode (BAS RE-5) were also placed in the electrochemical cell. Au was electrochemically deposited from an commercial aqueous plating solution (Orotemp 24, Technics) using a constant potential of -1 V vs. Ag/AgCl. The electrochemical deposition was performed using a PAR Model 173 potentiostat/galvanostat equipped with a PAR Model 179 digital coulometer. The length of the Au nanorods was changed by varying the deposition time.[15] The coulombs that were passed per cm^2 of exposed membrane area were monitored during the electrochemical deposition.

For Ag nanorods, an initial potential of -0.9 V vs. Ag/AgCl was used. This potential was decreased to -0.3 V vs. Ag/AgCl after ca. 5 mC cm^{-2} of Ag had been deposited. This slowed down the rate of Ag deposition so nanorods with reproducible lengths could be fabricated. The aqueous Ag plating solution was 0.09 M in $AgNO_3$ (Aldrich), 0.19 M in Na_2CO_3 (Mallinckrodt), 0.08 M in $K_4Fe(CN)_6 3H_2O$ (Mallinckrodt), and 1.54 M in KSCN (City Chemical Corp.).

After nanorod deposition, the Ag-film cathode was removed from the membrane surface by wiping with a laboratory tissue. Au nanorod-containing membranes were then immersed into a 50 % v/v solution of HNO_3 (Mallinckrodt) for 15 minutes to remove any residual Ag from the membrane. The membrane was then washed in H_2O and CH_3OH and dried in air. This acid-wash procedure was not used for the Ag nanorod-containing membranes.

Preparation of the Metal Nanorod Sols. The metal nanorod-containing template membrane was immersed into either 1,1,1,3,3,3-hexafluoro-2-propanol (HFIP) (Aldrich, 99+%) or $CHCl_3$ (Fisher Scientific, ACS grade) and manually shaken for ~10 s to dissolve the membrane. This also resulted in a dispersion of the freed nanorods into the solvent to form the sol. Unless otherwise stated, two circular pieces of membrane (45 mm diameter) were dissolved in this way into 10 mL of solvent. The mass of metal in each sol varied, of course, with both the diameter and the length of the suspended nanorods as well as with the identity of the metal (Au vs. Ag) (Table I). In addition, these sols contained ~24 mg of polycarbonate (PC) from the dissolved template membranes.

In some cases, a polymeric stabilizer was added to the nanorod sol. Stabilizers investigated were polyvinylpyrrolidone (PVP) (M.W. 40,000, Aldrich) and poly(2-Vinylpyridine) (P2VP) (M.W. 50,000, Polysciences). Unless otherwise stated, the stabilizer concentrations were 4 g L^{-1} for PVP and 26 g L^{-1} for P2VP. These concentrations were chosen in order to compare our results with those obtained by others for analogous template-prepared Au nanorod sols.[6]

Scanning Electron Microscopy (SEM). The lengths and diameters of the Au and Ag nanorods were determined using SEM. The SEM samples were prepared by filtering the sols through Anodisc 25 filtration membranes (0.2 μm pore diameter, Whatman). This left the nanorods on the surface of the filter. The filter was then washed with $CHCl_3$ to remove residual polycarbonate and sputtered with 5 nm of Au to prevent charging. The surface of the filter was then imaged using a Phillips 505 microscope. A typical image is shown in Figure 1.

While the nominal (i.e., specified by the provider) pore diameters were 10 and 30 nm, the diameter of the nanorods prepared in these membranes were larger (40 and 90 nm). This observation has been described previously.[12]

Characterization of the Metal Nanorod Sols. Nanometals show a characteristic absorbance in the visible region called the plasmon resonance absorption.[3,4] This absorbance provides a convenient route for characterizing the sols obtained. The stability of the sol was assessed by monitoring the magnitude of the absorbance as a function of time. In addition, the stability could be assessed by simply looking for precipitated Au at the bottom of the storage vial. Spectra were obtained carefully so as not to re-suspend this precipitated Au just before measurement. Data were obtained using a Hitachi U-3501 instrument.

RESULTS AND DISCUSSION

Aqueous colloidal dispersions of noble metal nanoparticles have been known for over 200 years. However, only recently have there been reports on the synthesis of noble metal colloids in organic solvents.[16-24] Spherical metal nanoparticles were prepared in this prior work. Rod-like colloids have been previously prepared for inorganic oxides such as imogolite (aluminosilicate),[25] boehmite (AlOOH),[26] and V_2O_5.[27] In addition, Au nanorod sols have been synthesized in aqueous solution.[6,7] These sols were shown to have interesting optical properties which varied with the aspect ratio of the nanorods. However,

neither of these reports focused on the long-term stability of these Au nanorod sols, and neither used organic solvents as was done here.

Table I shows the lengths, distribution of lengths, charge used during metal deposition, diameters, aspect ratios, and other relevant information about the Au and Ag nanorods investigated here. Note that, as would be expected, the aspect ratio increases with the quantity of charge used during metal deposition (C cm^{-2}). Throughout the remainder of this paper we will refer to these nanorods by specifying the diameter and the quantity of charge used during metal deposition.

Sols were prepared from these various nanorods using two different organic solvents - $CHCl_3$ and hexafluoroisopropanol (HFIP). The polycarbonate template membranes readily dissolve in these solvents, and this provides a route for both releasing the nanorods from the membrane and suspending the nanorods in these solvents. Au and Ag nanorods were investigated here because these nanorods have intense plasmon resonance absorption bands in the visible when dispersed within a porous solid, or in an aqueous or organic solvent.[2-4,15,28-33] The shape and position (energy) of this plasmon band is known to depend on the solvent (or solid) in which the nanorods are dispersed, the stabilizing polymer in the colloid (if any), the particle size, and the aspect ratio.[2-4,15,34-37] The intensity of this absorption band depends on the aspect ratio and diameter of the nanorods and on the quantity of metal suspended. As a result, the intensity of the plasmon band provides a convenient route for investigating the stability of these sols.

Au and Ag Nanorods Sols in $CHCl_3$ Without Stabilizers. Visually, the Ag nanorod sols had a yellow-green color, while the Au nanorod sols had either a pink (40 nm-dia.) or violet (90 nm-dia.) color. Representative absorption spectra for such $CHCl_3$-based metal nanorod sols are shown in Figure 2. Wavelength of maximum absorption intensity (λ_{max}) values obtained from such spectra are reported in Table I. These λ_{max} values are in good agreement with the reported plasmon resonance bands for both Au[21,24,38,39] and Ag [17,19,21,22,40,41] sols in organic solvents.

The λ_{max} values for the Au sols (Figure 2A) redshifted (from 524 nm to 553 nm) as the nanorod diameter was increased from 40 nm to 90 nm (Table I). This redshift in λ_{max} is in agreement with our prior solid-state investigations of such Au nanorods.[3,4] This expected redshift with increasing particle diameter was not seen for the Ag/$CHCl_3$ sols (Figure 2B). However, the absorption band for the 90 nm-dia. Ag sol (top spectrum, Figure 2B) was very broad and asymmetric. The tailing of this peak to longer wavelengths might be indicative of aggregation in this sol.[40] In addition, the 90 nm-diameter Ag nanorods had the largest dispersity in length (Table I). Such polydispersity can result in broadening of the plasmon band.[3]

The stability of these metal nanorod sols was studied by monitoring the absorption intensity at λ_{max} versus time. Figure 3A shows the stability of Ag nanorods of different diameters and aspect ratios in $CHCl_3$. As might be expected, the larger 90 nm-dia. nanorods (Figure 3A, Curves [3] and [4])

precipitated from the sol at a faster rate than the 40 nm-dia. Ag nanorods. Note that for these 40 nm-dia. sols, only ~20 % of the nanorods had precipitated from the sol after 90 hours. In addition, Figure 3C shows that after losing ~50 % of the initial amount of nanorods suspended, during a period of ~200 hours, no further loss was observed for a period of two months. In contrast, nearly all of the 90 nm-dia. Ag nanorods had precipitated from the sol after five days.

The Au nanorod sols had a slightly different trend in stability (Figure 3B). The longer 90 nm-dia. nanorods (Curve [4]) again precipitated from the sol at a faster rate than the 40 nm-dia. nanorods (Curves [1] and [2]). However, Figure 3B also indicates that the short (low aspect ratio) 90 nm-dia. Au nanorods (Curve [3]) had almost the same rate of precipitation as both of the 40 nm-dia. Au nanorods. These short 90 nm-dia. Au nanorods had the smallest aspect ratio of all of the Au nanorods studied here (see Table 1); therefore, it is not surprising that these sols would be almost as stable as the 40 nm-dia. Au sols. Interestingly, the 40 nm-dia. Au nanorod sols are less stable than the 40 nm-dia. Ag sols (compare Curves [1] and [2] in Figure 3A with Curves [1] and [2] in Figure 3B.) The 40 nm-dia. Au nanorod sols precipitated almost completely after seven days.

To further investigate the effect of aspect ratio on sol stability we compared the stabilities of sols prepared from 40 nm-dia. Au nanorods of four different aspect ratios (see Table I). The results are shown in Figure 4A. As the nanorod aspect ratio was increased, the stability of the sol decreased (e.g., Figure 4A Curve [4] vs. Curve [1]). The slopes of the linear portions (short times)

of these curves were determined by using least squares analysis to obtain the best fit line to each set of experimental data. This analysis showed that the highest aspect-ratio Au nanorods precipitated from the sol twenty times faster than the smallest aspect- ratio nanorods.

The effect of aspect ratio on the shape and λ_{max} value for the Au nanorod sols was also investigated (Figure 4B). As would be expected, the absorption intensity decreased from the longest (Spectrum [4]) to the shortest (Spectrum [1]) nanorod sols. Furthermore, a blueshift in λ_{max} was observed as the aspect ratio of the nanorods increased. We have previously seen such a blueshift with increasing aspect ratio in our solid-state investigations of such template-synthesized Au nanoparticles.[3]

The effect of concentration of the 40 nm-dia., 28.8 mC cm^{-2} Au nanorods on the stability of the sol was also investigated. Nanorod concentration was varied by adding one, two, three or four nanorod-containing template membranes to the same volume (10 mL) of $CHCl_3$. (The four-membrane sample contained ~0.16 mg Au mL^{-1}; the one-membrane sample contained ~0.04 mg Au mL^{-1}.) As shown in Figure 5, the most concentrated sol (Curve [4]) was less stable than the least concentrated one (Curve [1]). A comparison of the slopes, as before, showed that the concentration of nanorods in the most concentrated sol decayed three times faster than the concentration in the least concentrated sample. Furthermore, the absorption intensity at λ_{max} scaled with the concentration of nanorods in the sol. For example, the sample prepared from four membranes

had an initial absorption intensity of 0.76, and the sample prepared from one membrane had an initial absorption intensity of 0.19 .

Au and Ag Nanorod Sols in HFIP Without Stabilizers. Au and Ag nanorod sols were also prepared using HFIP as the solvent. The same general trend - faster precipitation of the high aspect-ratio 90 nm sols - was seen for both Ag and Au in HFIP. Furthermore, as was the case for $CHCl_3$, the low aspect-ratio 90 nm-dia. sol had approximately the same rate of precipitation as the 40 nm-dia. sols. It is also interesting to compare λ_{max} values for the HFIP and $CHCl_3$ sols (Table 1). Mie theory predicts that a blueshift should be observed as the refractive index of the solvent used is decreased.[36,42] The refractive indices of the solvents used here are 1.45 ($CHCl_3$) and 1.28 (HFIP). Table I shows that in agreement with Mie theory, the λ_{max} values for both the Au and Ag sols decrease with refractive index of the solvent.

Au and Ag Nanorod Sols with Added Stabilizers. Many noble metal colloids synthesized in organic solvents suffer from reduced stability relative to the analogous aqueous sol.[19,21,32,40,43] Recently, polymers have been added to the sols to enhance stability. For example, Ag sols in solvents such as ethanol, ethylene glycol, and toluene have been stabilized by adding poly(vinylpyrrolidone) (PVP), poly(vinylalcohol), or polystyrene to the sol.[20-22,44] Au colloids have been stabilized in CH_2Cl_2 and toluene by adding poly(vinylpyrrolidone), poly(vinylpyridine), and block copolymers of styrene and vinylpyridine to the sol.[16,21,24,45]

PVP was added at a concentration of 4 g L^{-1} to both the Au and Ag nanorod sols in HFIP. For Au nanorod sols, Figure 6 shows that the addition of PVP to the sols did not enhance the stability. For Ag nanorod sols, PVP was found to destabilize the sol relative to the analogous PVP-free sol. Indeed, the rate of precipitation of the Ag nanorods from the PVP-containing sol was dramatically higher than from the PVP-free sol. These data clearly show that PVP is not an effective stabilizer for these sols when HFIP is the solvent.

Figure 7 shows the effect of adding PVP or P2VP to the 40 nm-dia. Au sols (Figure 7A and 7B) and to the 90 nm-dia Au sols (Figure 7C and 7D). There is no clear indication that addition of either polymer appreciably stabilizes these sols. Analogous results were obtained for the Ag sols. In addition, the effect of the concentration of PVP on the stability of 90 nm-dia. Au nanorod sols was investigated. The concentration of added PVP was varied from 1 g L^{-1} to 32 g L^{-1}. The stability of these Au nanorod sols did not appreciably change with any of the studied PVP concentrations. Again, this result confirms that the addition of this polymer does not appreciably change the stability of these sols.

CONCLUSIONS

These studies have shown that reasonably stable Ag and Au nanorod sols can be prepared from the 40 nm-dia. nanorods. As might be expected, smaller aspect-ratio nanorod sols have greater stability than sols prepared from higher aspect-ratio nanorods. Furthermore, higher nanorod-concentration sols had lower stability. Finally, the polymeric stabilizers PVP and P2VP did not enhance stability of these sols.

This later point is of some interest because stabilization with P2VP was observed for Au nanorods template-synthesized in microporous alumina membranes.[6] One possible explanation for this apparent discrepancy between Au nanorods prepared in polycarbonate and Au nanorods prepared in alumina is that the polycarbonate itself is acting as a stabilizer. To our knowledge polycarbonate has never been used as a polymeric stabilizer for metal sols. However, because the pores in these membranes are prepared via hydrolysis of the polycarbonate, oxyanionic sites are present on the pore walls, and these sites may chemisorb to the surfaces of the metal nanorods.

This possibility is supported by the fact that recent X-ray photoelectron spectroscopic studies showed that PVP can interact with Ag nanoparticles through the oxygen atom in the carbonyl group of the polymer.[46] Analogous results were obtained for Ag nanoparticles and poly(vinylacetate).[47] We are suggesting a similar O-metal interaction for polycarbonate. If this is correct then polycarbonate is perhaps acting as a polymer stabilizer or these nanorods.

ACKNOWLEDGMENTS.

This work was supported by the Office of Naval Research and the Department of Energy. We would also like to thank the CSU Electron Microscopy Center for access to the microscopy equipment. In addition, VMC would also like to thank David Miner, Erin Crosthwait, and Kim Jackson for initial work dealing with this project.

FIGURE CAPTIONS

Figure 1 Scanning electron micrographs of Au nanorods filtered from the sols. (A) 40 nm-dia. nanorods electrochemically deposited using 14.4 mC cm^{-2}. (B) 40 nm-dia. nanorods electrochemically deposited using 28.8 mC cm^{-2}. (C) 90 nm-dia. nanorods electrochemically deposited using 14.4 mC cm^{-2}. (D) 90 nm-dia. nanorods electrochemically deposited using 28.8 mC cm^{-2}.

Figure 2 Visible spectra of 40 nm-dia. (———) and 90 nm-dia. (- - - -) Au (A) and Ag (B) nanorod sols in $CHCl_3$ (without additional polymeric stabilizers). In both (A) and (B), 28.8 mC cm^{-2} of metal were electrochemically deposited into the pores of each template membrane. The spectra were taken four hours after the sols were prepared.

Figure 3 (A) Plot of absorbance vs. time (stability plot) of sols containing Ag nanorods of different diameters and aspect ratios in $CHCl_3$. No additional polymeric stabilizers were added. Sols are listed as follows: (1) 40 nm-dia., 14.4 mC cm^{-2} (2) 40 nm-dia., 28.8 mC cm^{-2} (3) 90 nm-dia., 14.4 mC cm^{-2} (4) 90 nm-dia., 28.8 mC cm^{-2}. (B) Analogous plot for Au nanorods in $CHCl_3$. Sols are listed as follows: (1) 40 nm-dia., 14.4 mC cm^{-2} (2) 40 nm-dia., 28.8 mC cm^{-2} (3) 90 nm-dia., 14.4 mC cm^{-2} (4) 90 nm-dia., 28.8 mC cm^{-2}. (C) Long-term stability of the 40 nm-dia., 28.8 mC cm^{-2} Ag sol.

Figure 4 (A) Plot of absorbance vs. time (stability plot) of sols containing four different aspect-ratio 40 nm-dia. Au nanorods in $CHCl_3$. Sols are listed as follows: (1) 14.4 mC cm^{-2} (2) 28.8 mC cm^{-2} (3) 57.7 mC cm^{-2} (4) 115.3 mC cm^{-2}. (B) Visible absorbance spectra of the sols shown in (A). The sols from bottom to top are: (1) 14.4 mC cm^{-2} (2) 28.8 mC cm^{-2} (3) 57.7 mC cm^{-2} (4) and 115.3 mC cm^{-2} of Au electrochemically deposited, respectively.

Figure 5 Plot of absorbance vs. time (stability plot) for 40 nm-dia. Au sols in $CHCl_3$ (28.8 mC cm^{-2} of Au deposited) at various concentrations of the nanorods. No additional polymeric stabilizers were added. Sols are identified as follows: (1) One template membrane per 10 mL of $CHCl_3$. (2) Two membranes per 10 mL of $CHCl_3$. (3) Three membranes per 10 mL of $CHCl_3$. (4) Four membranes per 10 mL of $CHCl_3$.

Figure 6. Plot of absorbance vs. time for various Au nanorods in HFIP with and without added PVP. (A) 40 nm-dia. Au sols. (1) 14.4 mC cm^{-2} without PVP (2) 14.4 mC cm^{-2} with PVP (3) 28.8 mC cm^{-2} without PVP (4) 28.8 mC cm^{-2} with PVP. (B) Analogous data for 90 nm-dia. Au sols in HFIP. The plot labels are identical to those in (A).

Figure 7. Plots of absorbance vs. time for 40 nm-dia. and 90 nm-dia. Au sols with and without the addition of the stabilizers PVP and P2VP in $CHCl_3$. (A) 40 nm-dia., 14.4 mC cm^{-2}. (B) 40 nm-dia., 28.8 mC cm^{-2}. (C) 90 nm-dia., 14.4 mC cm^{-2}. (D) 90 nm-dia., 28.8 mC cm^{-2}.

REFERENCES

1) Hulteen, J. C.; Martin, C. R. *J. Mater. Chem.* **1997**, *7*, 1075.

2) Martin, C. R. *Science* **1994**, *266*, 1961.

3) Hornyak, G. L.; Patrissi, C. J.; Martin, C. R. *J. Phys. Chem. B* **1997**, *101*, 1548.

4) Hornyak, G. L.; Martin, C. R. *Thin Solid Films* **1997**, *303*, 84.

5) De Vito, S.; Martin, C. R. *Chem. Mater.* **1998**, *7*, 1738.

6) van der Zande, B. M. I.; Böhmer, M. R.; Fokkink, L. G. J.; Schönenberger, C. *J. Phys. Chem. B* **1997**, *101*, 852.

7) Yu, Y.-Y.; Chang, S.-S.; Lee, C.-L.; Wang, C. R. C. *J. Phys. Chem. B* **1997**, *101*, 6661.

8) Jirage, K. B.; Hulteen, J. C.; Martin, C. R. *Science* **1997**, *278*, 655.

9) Menon, V. P.; Martin, C. R. *Anal. Chem.* **1995**, *67*, 1920.

10) Nishizawa, M.; Menon, V. P.; Martin, C. R. *Science* **1995**, *268*, 700.

11) Whitney, T. M.; Jiang, J. S.; Searson, P. C.; Chien, C. L. *Science* **1993**, *261*, 1316.

12) Schönenberger, C.; van der Zande, B. M. I.; Fokkink, L. G. J.; Henny, M.; Schmid, C.; Krüger, M.; Bachtold, A.; Huber, R.; Birk, H.; Stafer, U. *J. Phys. Chem. B* **1997**, *101*, 5497.

13) Brumlik, C. J.; Martin, C. R. *J. Am. Chem. Soc.* **1991**, *113*, 3174.

14) Brumlik, C. J.; Menon, V. P.; Martin, C. R. *J. Mater. Res.* **1994**, *9*, 1174.

15) Foss, C. A.; Tierney, M. J.; Martin, C. R. *J. Phys. Chem.* **1992**, *96*, 9007.

16) Antonietti, M.; Wenz, E.; Bronstein, L.; Sergegina, M. *Adv. Mater.* **1995**, *7*, 1000.

17) Cardenas-Trivino, G.; Vera L, V.; Muñoz, C. *Mater. Res. Bull.* **1998**, *33*, 645.

18) Devenish, R. W.; Goulding, T.; Heaton, B. T. *J. Chem. Soc. Dalton Trans.* **1996**, *1996*, 673.

19) Garrell, R. L.; Schultz, R. H. *J. Colloid Interface. Sci.* **1985**, *105*, 483.

20) Hirai, H. *J. Macromol. Sci.-Chem.* **1979**, *A13 (5)*, 633.

21) Klabunde, K. J.; Habdas, J.; Cárdenas-Triviño, G. *Chem. Mater.* **1989**, *1*, 481.

22) Siiman, O.; Lepp, A.; Kerker, M. *Chem. Phys. Lett.* **1983**, *100*, 163.

23) Silvert, P.-Y.; Herrera-Urbina, R.; Duvauchelle, N.; Vijayakrishnan, V.; K, T., Elhsissen *J. Mater. Chem.* **1996**, *6*, 573.

24) de Caro, D.; Agelou, V.; Duteil, A.; Chaudret, B.; Mazel, R.; Roucau, C.; Bradley, J. S. *New J. Chem.* **1995**, *19*, 1265.

25) Donkai, N.; Inagaka, H.; Kajiwara, K.; Urakawa, H.; Schmidt, M. *Macromol. Chem.* **1985**, *186*, 2623.

26) Buining, P. A.; Pathmamanoharan, C.; Jansen, J. B. H.; Lekkerkerker, H. N. W. *J. Am. Ceram. Soc.* **1991**, *74*, 1303.

27) Zocher, H. *Z. Anorg. Chem.* **1925**, *147*, 91.

28) Creighton, J. A.; Blatchford, C. G.; Albrecht, M. G. *Faraday Trans. II* **1979**, *5*, 790.

29) Henglein, A. *J. Phys. Chem.* **1993**, *97*, 5457.

30) Chumanov, G.; Sokolov, L.; Gregory, B. W.; Cotton, T. M. *J. Phys. Chem.* **1995**, *99*, 9466.

31) Liz-Marzán, L. M.; Lado-Touriño, I. *Langmuir* **1996**, *12*, 3585.

32) Zeiri, L.; Efrima, S. *J. Phys. Chem.* **1992**, *96*, 5908.

33) Underwood, S.; Mulvaney, P. *Langmuir* **1994**, *10*, 3427.

34) Turkevich, J.; Stevenson, P. C.; Hillier, J. *J. Discuss. Faraday Soc.* **1951**, *11*, 55.

35) Turkevich, J.; Garton, G.; Stevenson, P. C. *J. Colloid Sci.* **1954**, *9*, 26.

36) Bohren, C. F.; Huffman, D. F. *Absorption and Scattering of Light by Small Particles*; Wiley: New York, 1983.

37) Kerker, M. *The Scattering of Light and Other Electromagnetic Radiation*; Academic Press: New York, 1969.

38) Antonietti, M.; Thünemann, A.; Wenz, E. *Colloid Polym. Sci.* **1996**, *274*, 795.

39) Satoh, N.; Hasagawa, H.; Tsujii, K. *J. Phys. Chem.* **1994**, *98*, 2143.

40) Wang, W.; Efrima, S.; Regev, O. *Langmuir* **1998**, *14*, 602.

41) Kang, S. Y.; Kim, K. *Langmuir* **1998**, *14*, 226.

42) Doremus, R. H. *J. Appl. Phys.* **1964**, *35*, 2456.

43) Lin, S.-T.; Franklin, M. T.; Klabunde, K. J. *Langmuir* **1986**, *2*, 259.

44) Marzán, L. L.; Philipse, A. P. *Colloids and Surfaces A* **1994**, *90*, 95.

45) Roescher, A.; Möller, M. *Adv. Mater.* **1995**, *7*, 151.

46) Huang, H. H.; Ni, X. P.; Loy, G. L.; Chew, C. H.; Tan, K. L.; Loh, F. C.; Deng, J. F.; Xu, G. Q. *Langmuir* **1996**, *12*, 909.

47) Zimmerman, F.; Wokaun, A. *Prog. Coll. Polym. Sci.* **1990**, *81*, 242.

Table 1 Characteristics of the Au and Ag Nanorod Sols Prepared in $CHCl_3$ and HFIP

Nanorod Diameter (nm)[a]	Charge Passed ($mC\ cm^{-2}$)[b]	Nanorod Length (μm)[a]	Nanorod Aspect Ratio (Length/Diameter)	λ_{max} (nm)[c] (CHCl3)	λ_{max} (nm)[c] (HFIP)	mg mL^{-1} of Metal in Sol
Au						
40 ± 10	14.4	0.7 ± 0.2	18	527	516	0.02
40 ± 10	28.8	1.1 ± 0.3	28	524	512	0.08
40 ± 10	57.7	2.2 ± 0.5	57	523	-------	------
40 ± 10	115.3	2.4 ± 1.1	61	520	-------	------
90 ± 20	14.4	0.4 ± 0.1	5	539	524	0.04
90 ± 20	28.8	0.6 ± 0.1	7	553	532	0.11
Ag						
40 ± 10	14.4	2.7 ± 0.5	66	395	368	0.05
40 ± 10	28.8	3.5 ± 0.6	87	395	368	0.14
90 ± 20	14.4	0.9 ± 0.2	10	394	383	0.13
90 ± 20	28.8	1.7 ± 0.3	18	392	382	0.17

[a] Nanorod diameters and lengths were obtained from scanning electron micrographs similar to those shown in Figure 4.2 and 4.3.

[b] Charge passed was based on an electrode area of 17.34 cm^2.

[c] λ_{max} was determined to have a standard deviation of ± 2.5 nm.

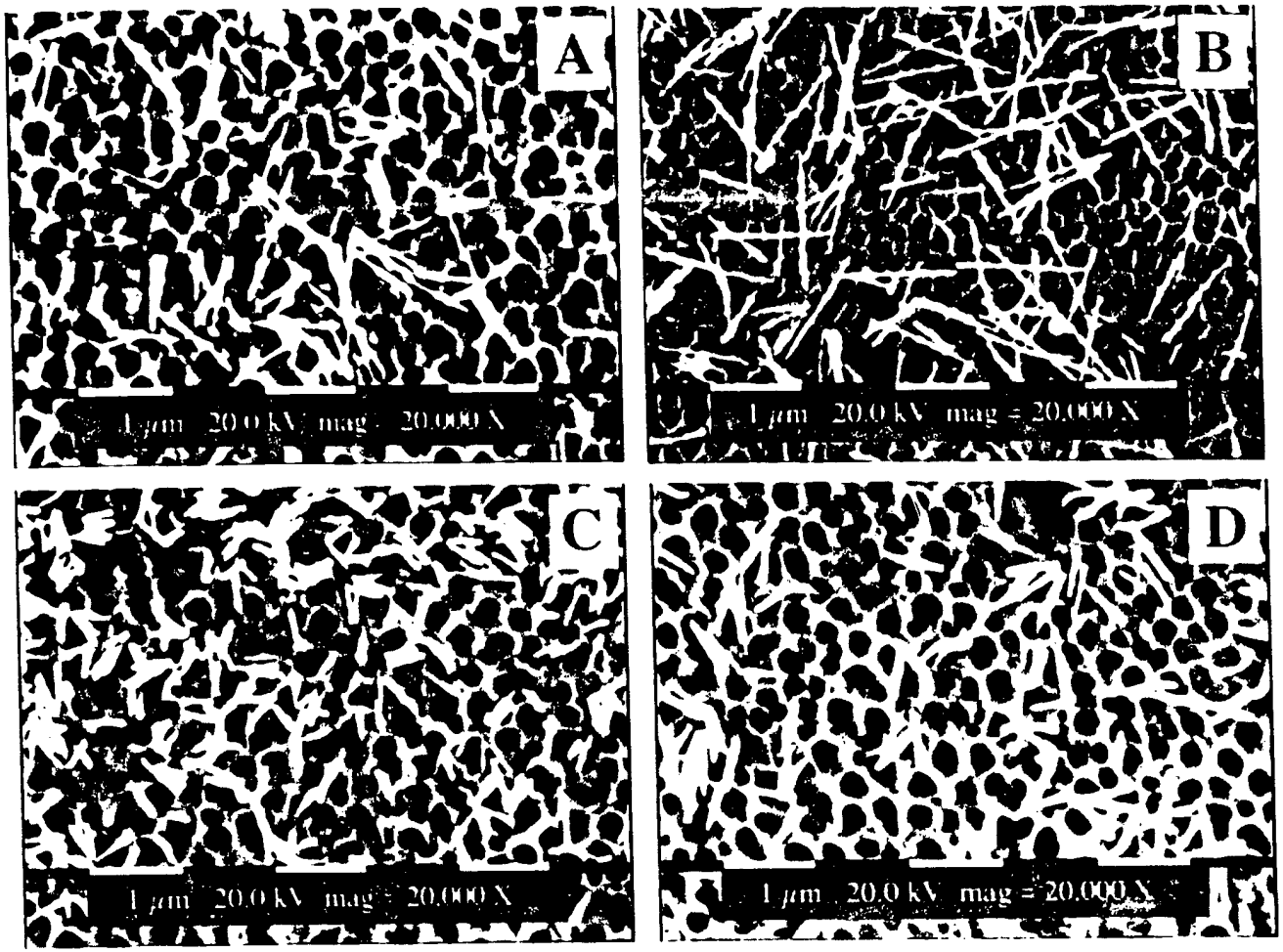
A
1 μm 20.0 kV mag = 20,000 X
B
1 μm 20.0 kV mag = 20,000 X
C
1 μm 20.0 kV mag = 20,000 X
D
1 μm 20.0 kV mag = 20,000 X

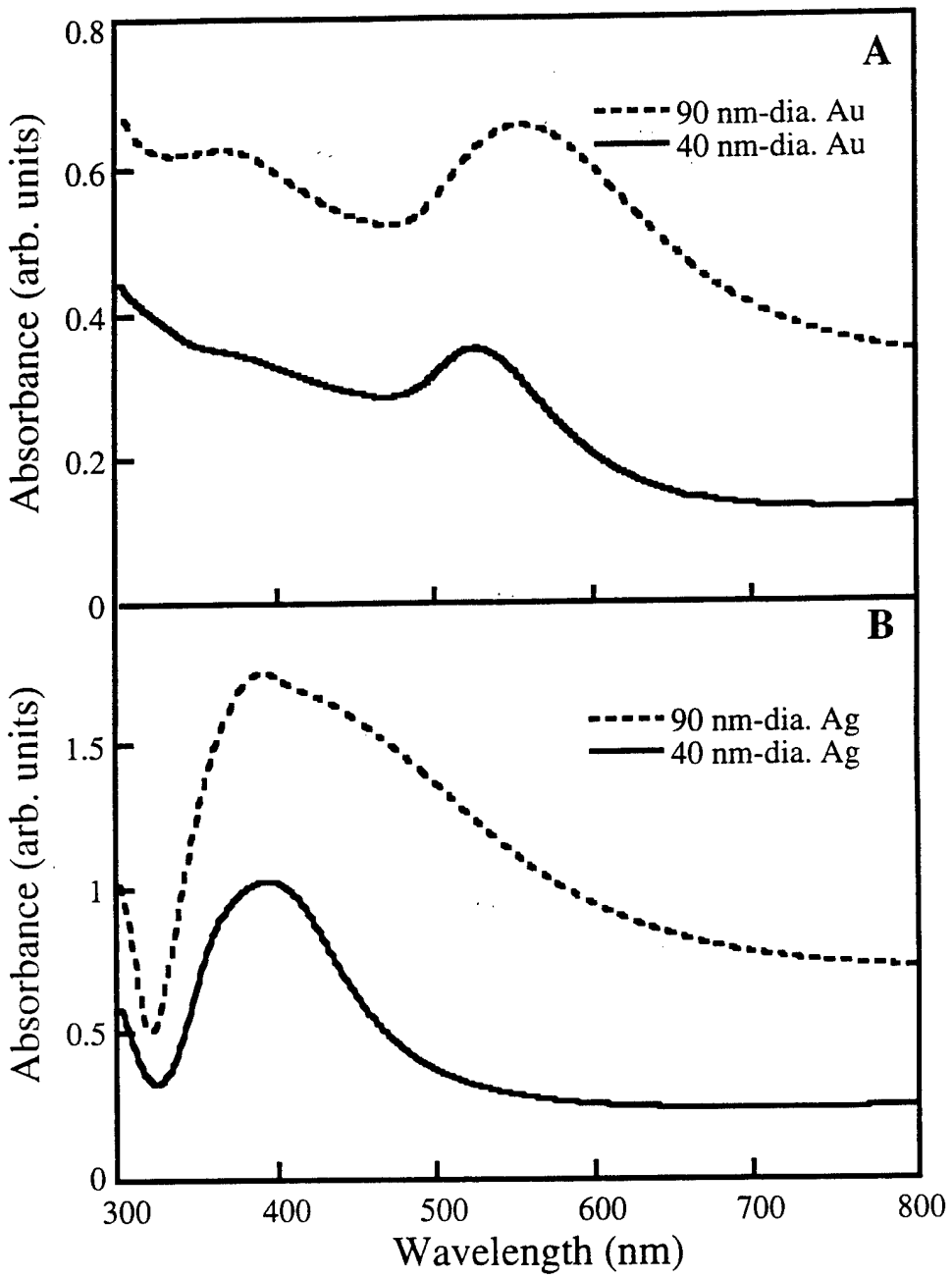
A
90 nm-dia. Au
40 nm-dia. Au
Absorbance (arb. units)
0.8
0.6
0.4
0.2
0
B
90 nm-dia. Ag
40 nm-dia. Ag
Absorbance (arb. units)
1.5
1
0.5
0
300
400
500
600
700
800
Wavelength (nm)

Fig 2

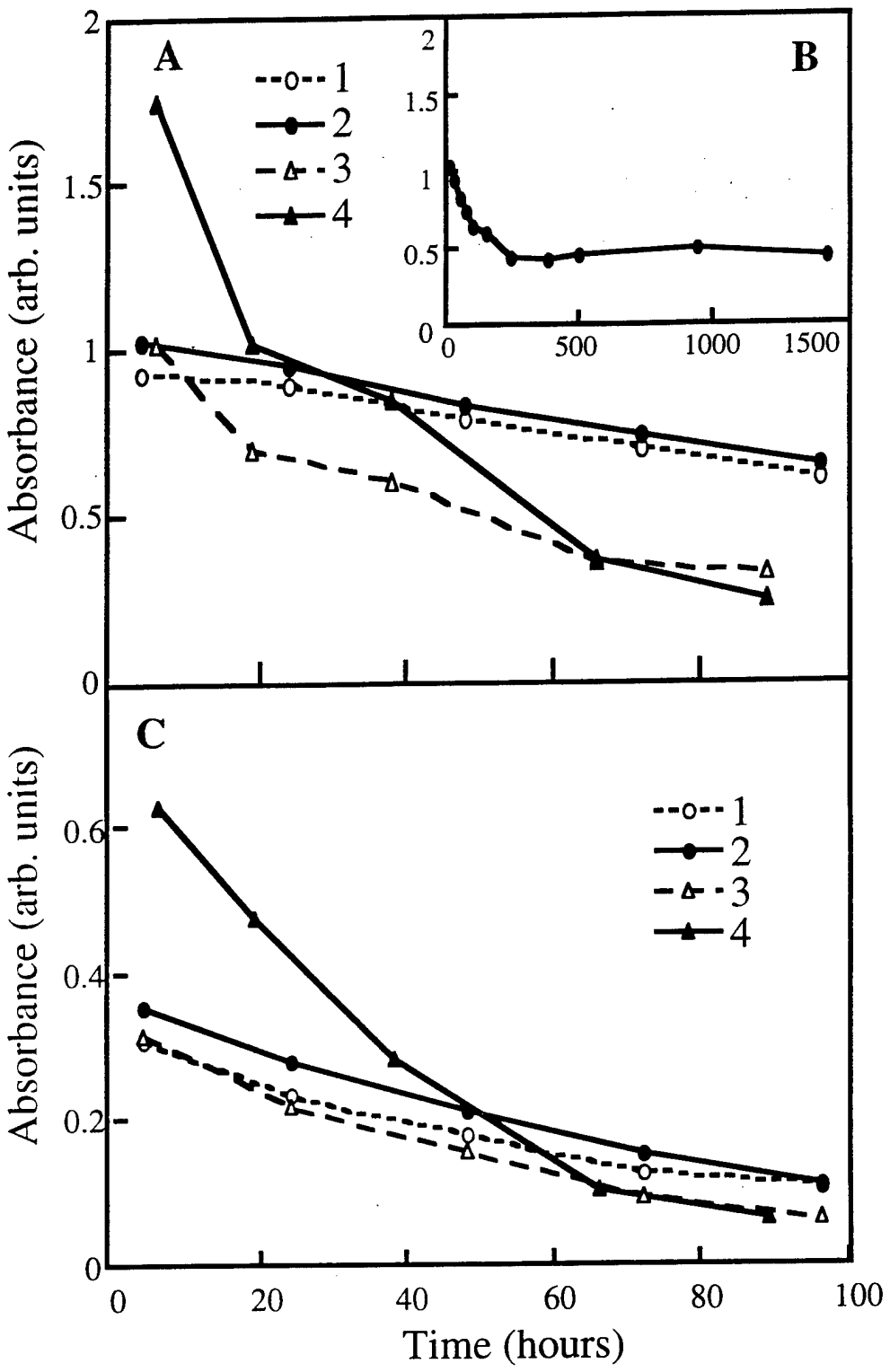
A
B
C
1
2
3
4
Absorbance (arb. units)
Absorbance (arb. units)
Time (hours)
0
0.5
1
1.5
2
0
500
1000
1500
0.2
0.4
0.6
0
20
40
60
80
100

Fig 3

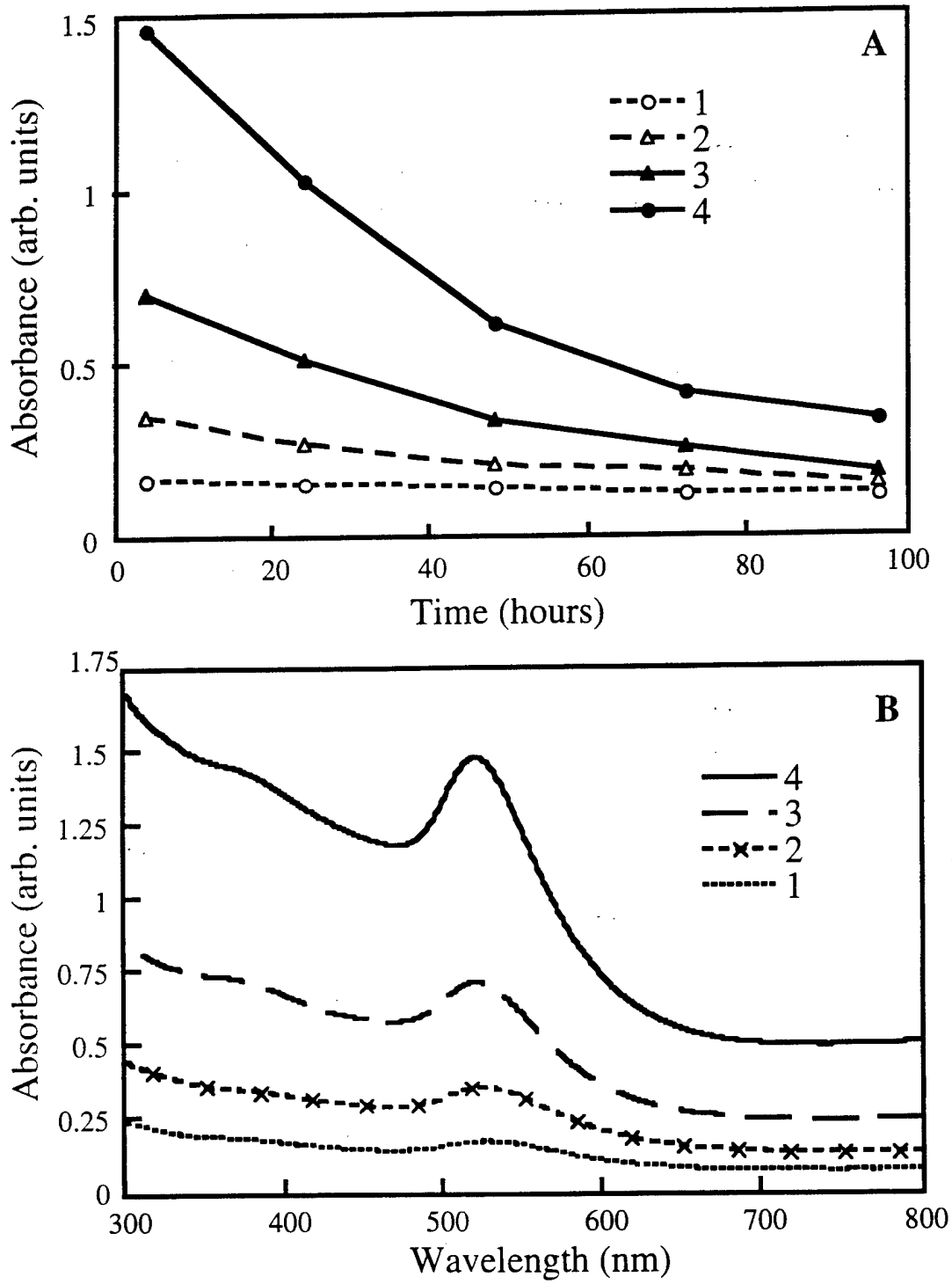
A
1
2
3
4
Absorbance (arb. units)
Time (hours)
0
0.5
1
1.5
0
20
40
60
80
100
B
4
3
2
1
Absorbance (arb. units)
Wavelength (nm)
0
0.25
0.5
0.75
1
1.25
1.5
1.75
300
400
500
600
700
800

Fig 4

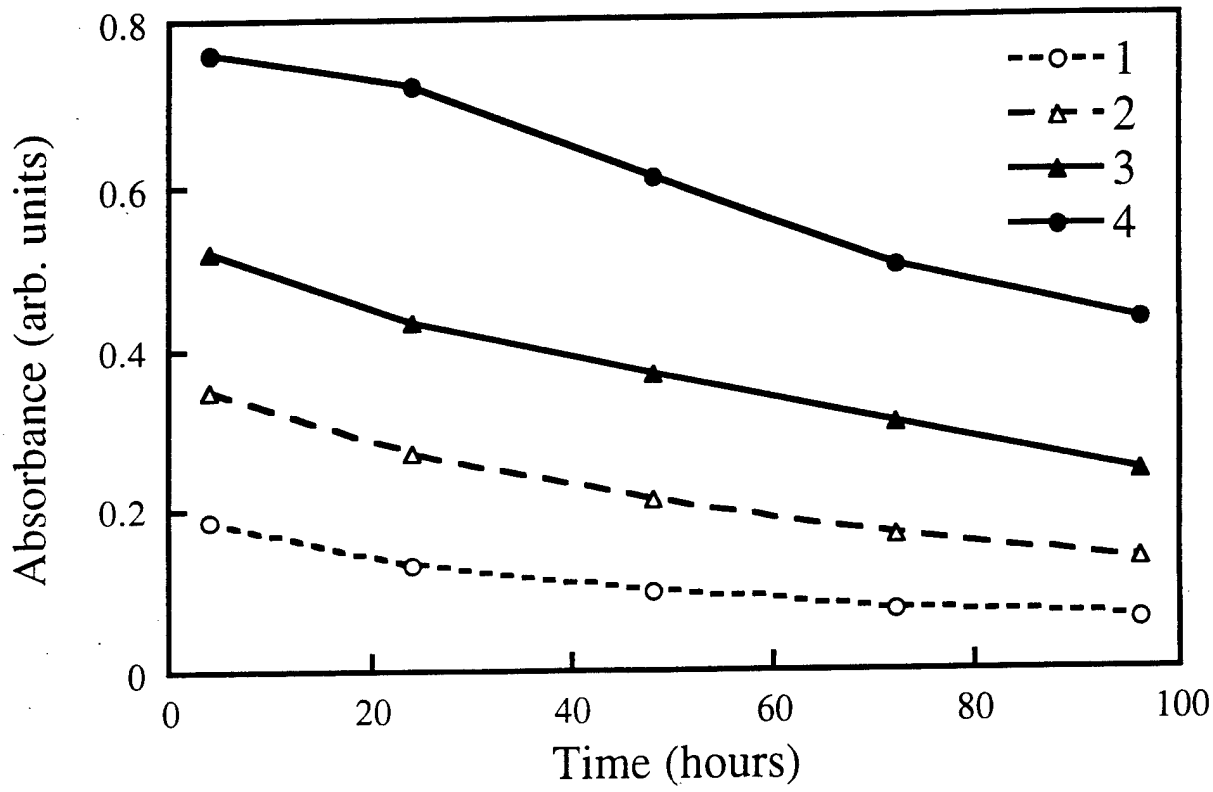
0.8
0.6
0.4
0.2
0
Absorbance (arb. units)
0
20
40
60
80
100
Time (hours)
1
2
3
4

Fig 5

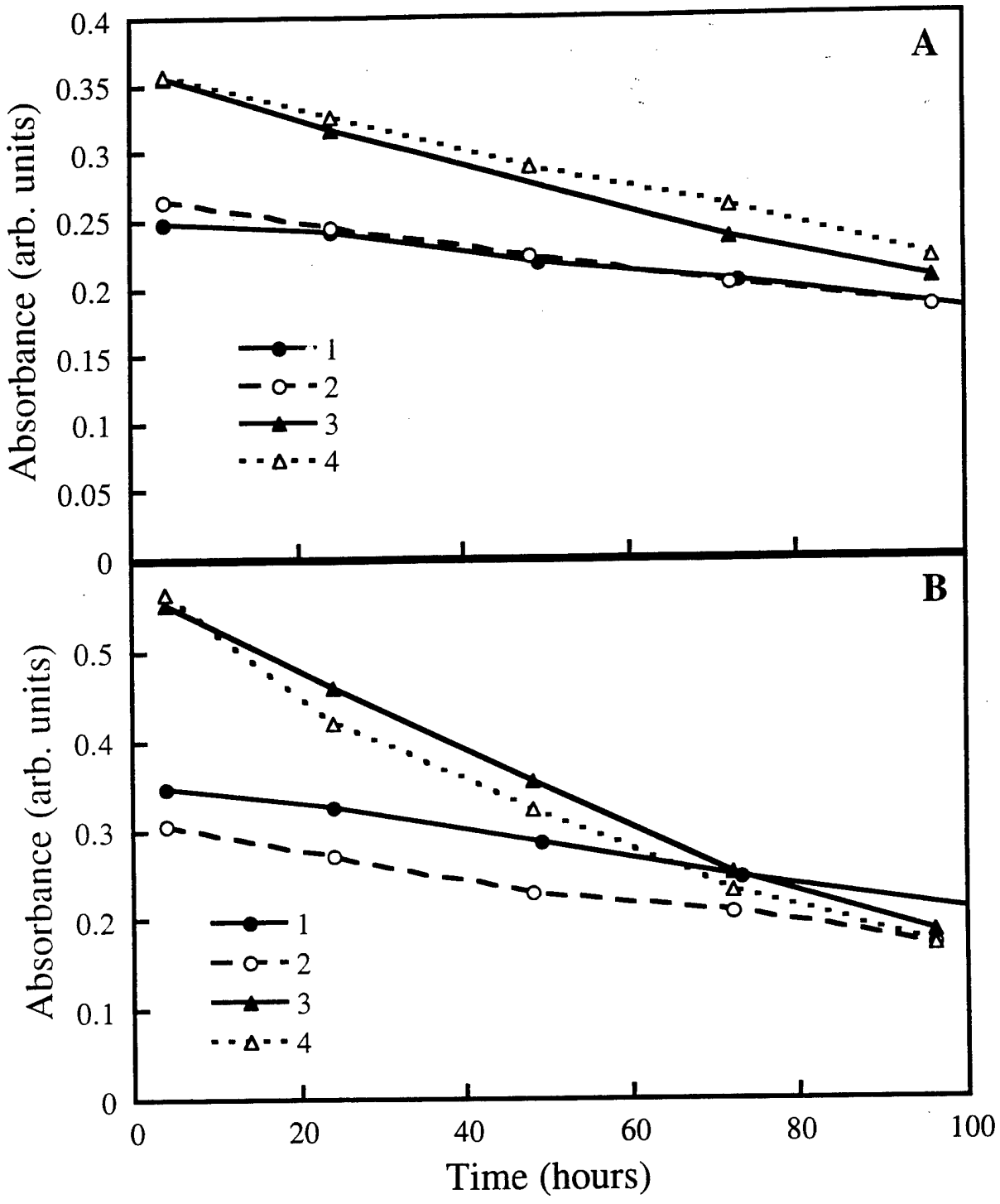
A
B
Absorbance (arb. units)
Absorbance (arb. units)
0.4
0.35
0.3
0.25
0.2
0.15
0.1
0.05
0
0.5
0.4
0.3
0.2
0.1
0
1
2
3
4
1
2
3
4
0
20
40
60
80
100
Time (hours)

Fig 6

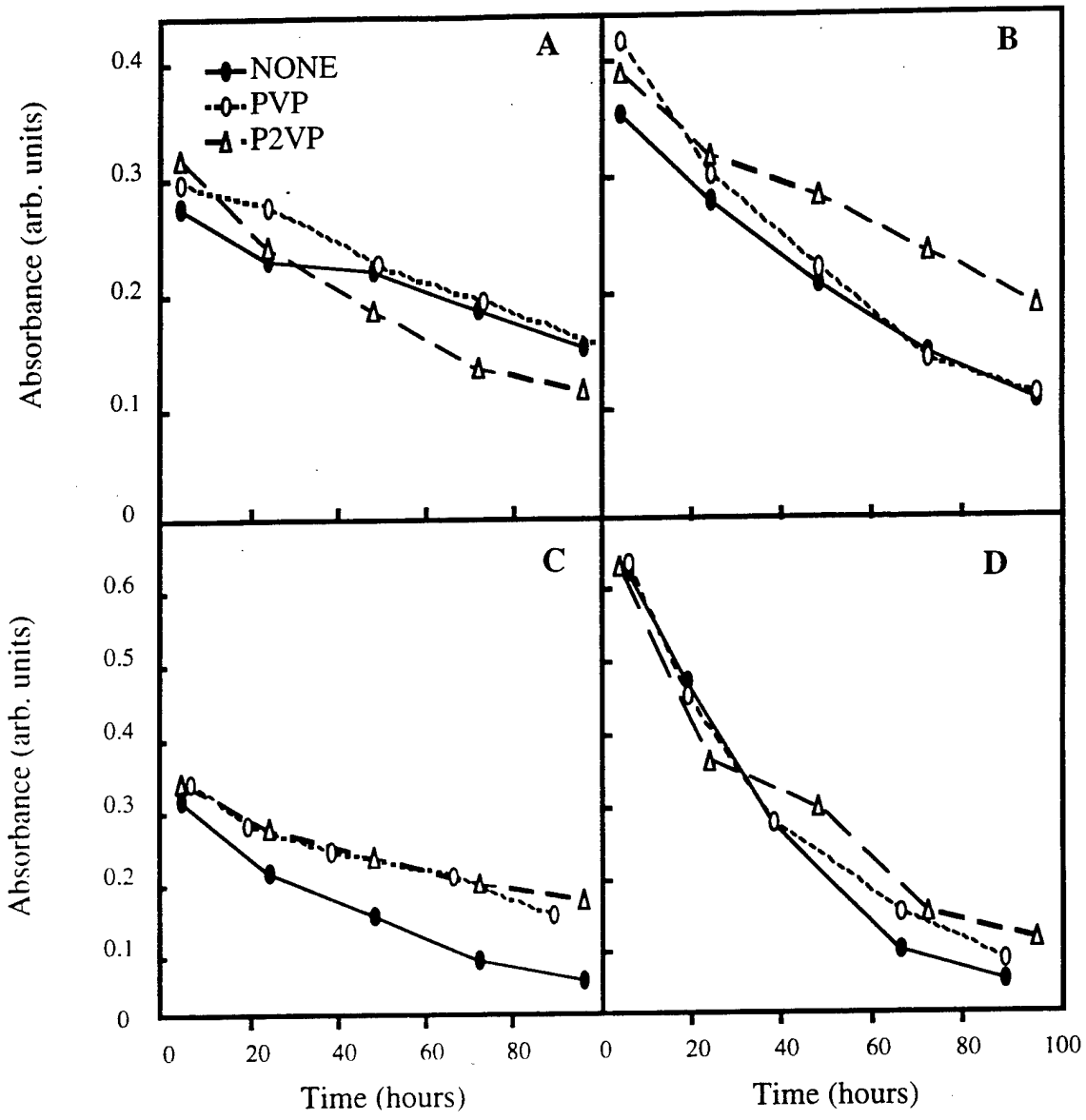
A
B
C
D
NONE
PVP
P2VP
Absorbance (arb. units)
Absorbance (arb. units)
0.4
0.3
0.2
0.1
0
0.6
0.5
0.4
0.3
0.2
0.1
0
0
20
40
60
80
0
20
40
60
80
100
Time (hours)
Time (hours)

Fig 7